Research Paper

Effects of surface geology and topography on the damage severity during the 2015 Nepal Gorkha earthquake

K. Sharma [1], M. Subedi [2], R.R. Parajuli [3] and B. Pokharel [4]

ARTICLE INFORMATION

ABSTRACT

An earthquake of moment magnitude (M_w) 7.8 struck Nepal at 06:11 UTC on April 25, 2015. A field reconnaissance was carried out immediately after the main shock. This paper presents the accelerograms and the geology of Nepal. The acceleration response spectra of the motions at the valley show a prominent amplification at the period of 5 sec. This paper describes the effects of local geology and topography on the damage severity during the earthquake. The damage patterns illustrate the strong influence of local geology conditions on the severity of the damage at many places, like soil amplification in Gongabu, Machhapokhari, Ramkot, Purano Naikap, areas along the major rivers in Kathmandu Valley with loose alluvium deposits, and ridge effects on the Swayambhu Nath hill and Chautara. The effect of low frequency amplification caused by the Kathmandu Valley basin is evident from the severe damage to well-designed tall buildings in Kathmandu. Severe damages including ground fissures and liquefactions were observed adjacent to basin edges around the Kathmandu Valley. It was concluded on the basis of the observation that local geology, rather than engineering features of structures, largely determined the severity of damage during the earthquake.

1. Introduction

On April 25, 2015, a moment magnitude (M_w) 7.8 earthquake struck near Kathmandu, Nepal and was followed by a series of large aftershocks, including a further moment magnitude (M_w) 7.3 on May 12. The epicenter (N: 28.1470°; E: 84.7080°) of the main shock was located about 77 km northwest of Kathmandu at a focal depth of approximately 15 km (USGS, 2015). A total of 800,000 buildings were severely damaged or collapsed (Sharma et al., 2016; Manandhar et al., 2016). The earthquake caused a heavy toll of about 9,000 dead, more

than 23,000 injured, and more than U.S. $5.0 billion in losses. These seismic events in the central Himalaya were the strongest after the 1934 earthquake that was located northeast of Kathmandu (Bilham et al., 2001). As of November 30, 2016, a total of 470 aftershocks with a magnitude above 4 had been observed, 49 with a magnitude above 5, and 5 above 6 (NSC, 2016).

It has been accepted that, besides the earthquake magnitude and distance from fault, local site conditions (geological condition and topography), known as site effects, can impose significant influences on the earthquake ground motion at a given place. Site effects

[1] PhD student, Department of Civil and Environmental Engineering, University of Alberta, Alberta, CANADA, keshab@ualberta.ca
[2] PhD student, Department of Civil Engineering, Central Campus, Institute of Engineering, Lalitpur, NEPAL, subedimandip@gmail.com
[3] PhD student, Earthquake and Lifeline Engineering Laboratory, Department of Urban Management, Kyoto University, Kyoto, JAPAN, parajuli.ram.27z@st.kyoto-u.ac.jp
[4] Former student, National College of Engineering, Tribhuvan University, Lalitpur, NEPAL, bigulpokhrel@gmail.com
Note: Discussion on this paper is open until September 2017

have been widely observed in previous earthquakes. Previous earthquakes such as the Northridge earthquake (1994), Kobe earthquake (1995), Bhuj earthquake (2001), Kashmir earthquake (2005), Sichuan earthquake (2008), Chile earthquake (1985), and the Haiti earthquake (2010) have depicted the role of local site conditions on earthquake damage (Rayhani, 2008; Hough et al., 2010; Celebi, 1987; Sharma and Deng, 2017). Local site effects owing to geological conditions was observed during the 1989 Loma Prieta earthquake. Two sites were both situated around 80 km from the earthquake epicenter, but the soft-soil site experienced a much higher acceleration than the rock site. The peak ground acceleration recorded at the soft site was 0.220 g, whereas that at the rock site was 0.090 g (Villaverde, 2009). Damage patterns in Mexico City after the 1985 Michoacan earthquake demonstrated conclusively the significant effects of local site conditions on the seismic ground response. Site effects due to topographic condition (also known as ridge effect) was profound during 1985 Chile earthquake, the houses on hill tops or ridges were heavily damaged whereas those on nearly flat sites were only slightly damaged (Villaverde, 2009).

Several studies have reaffirmed the amplification of ground motion and comparatively severe earthquake damage in the Kathmandu Valley due to the subsoil structure of the valley (Hough and Bilham, 2008; Pandey and Molnar, 1988; Mugnier et al., 2011; Paudyal et al., 2012). Based on the evidence of damage severity in the

valley during past earthquakes, including 1934 Bihar-Nepal earthquake, Dixit et al. (2000), Hough and Bilham (2008), and Mugnier et al. (2011) have concluded that the valley is characterized by strong site effects. Microtremor studies in Kathmandu Valley (Paudyal et al., 2012) also highlighted strong site effects in the Kathmandu Valley. Soil thickness and material properties in the valley vary from place to place, which may cause trapping and focusing of seismic waves during an earthquake, leading to an evident change in ground motion characteristics over short distances.

A field reconnaissance of the 2015 Nepal Gorkha earthquake was carried out immediately after the main shock. The main purpose of this article is to investigate the role of local site conditions over the degree and distribution of the structural and geotechnical damage in the devastated area and to offer lessons of this destructive earthquake. In this paper, geology of Nepal is briefly described and the recorded ground motions are characterized. This paper discusses the observed damage severity due to local site effects in Kathmandu Valley and nearby region. Observed case studies of local site effects are also presented.

2. Plate tectonic and geology of Nepal

The 2,400 km long Himalayan Mountain range was formed by the collision of Indian plate and Eurasian plate
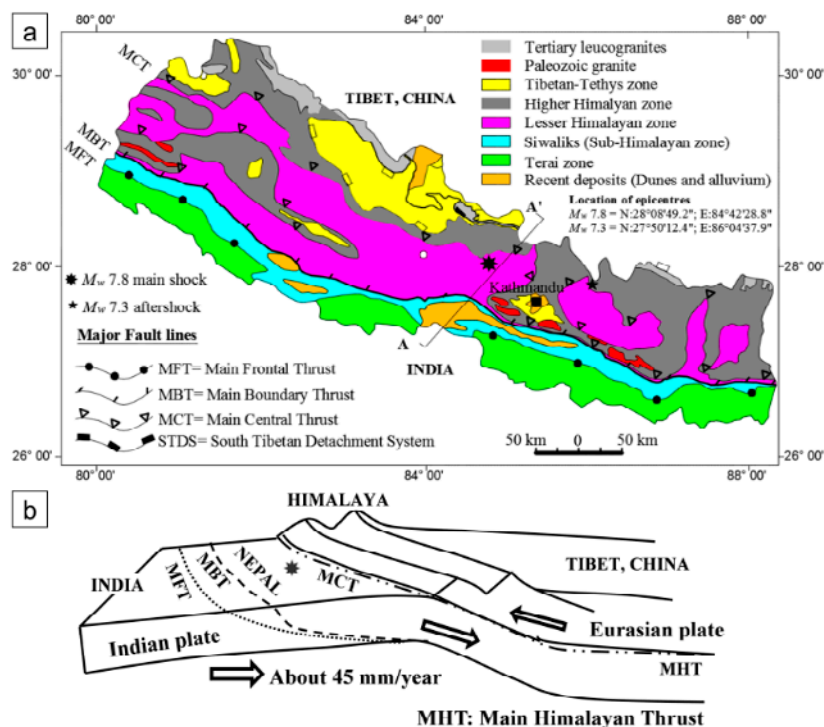
Fig. 1. (a) Tectonic zoning of Nepal with active faults (modified after Dahal (2006) and locations of the main shock and M_w 7.3 aftershock, and (b) motion and type of plate boundaries at the cross section A-A' (Sharma and Deng, 2017).

starting 40 million years ago. Nepal is situated in the center of the Himalayan concave chain and is rectangular in shape of about 900 km in the NWW-SEE and 130 to 260 km in N-S direction. The Himalayan arc, which is one of the most active seismic regions on earth, has caused numerous major earthquakes in past centuries (Bilham et al., 2001; Ambraseys and Douglas, 2004). **Figure 1a** shows the tectonic zones, major faults, and geologic map of Nepal. The 2015 Gorkha earthquake was the result of thrust faulting between the subducting India plate and the Eurasia plate to the north (**Fig. 1b**), where the Indian plate converges with the Eurasian plate at a rate of 45 mm per year towards the north-northeast (Copeland, 1997).

Figure 2 shows the geologic map of the Kathmandu Valley, where the majority of the observations in this studies are located. Geological study has shown that the Kathmandu Valley is an ancient lake deposit and is made of thick layers of clay, silt, sand, and gravel. The maximum thickness of the valley soil is 500-550 m at the center of the valley (Sakai et al., 2002). As shown in **Fig. 2**, the valley south soils consists of boulders and gravel with a clayey and silty matrix derived as debris flows from the southern hill, while marginal fluvio-deltaic facies (i.e., typical riverbed layered deposits of clays, silts, sand, and gravels) are found in the valley north, and the central basin consists of open lacustrine facies (e.g., thick organic mud, and the black clay). As the soil deposited in irregular layers, soil properties and basin thickness vary from place to place.

In order to characterize the subsurface soil properties, few representative standard penetration tests (SPT) were carried out at five selected sites in the Kathmandu Valley; disturbed soil samples were obtained with the SPT for laboratory soil characterization. The SPT sites were chosen because they are readily available and near the liquefied or severely devastated areas. The sites are primarily located in regions of the fluvio–deltaic facies and the fan deposits. In the absence of geophysical tests, the shear wave velocity (V_s) was estimated through the correlation with corrected SPT values, proposed by JICA, for the alluvial deposit of the Kathmandu Valley ($Vs = 97*N^{1/3}$; N = SPT N value) for all types of soils (JICA, 2002). According to this correlation, V_s varies from 150 to 350 m/s in the valley. Five representative borehole logs with the shear wave profile are presented in **Fig. 3**.

The site investigation showed that most soils in the Kathmandu Valley are grey to dark silty sand and clayey silt. Organic clay, fine sand beds and peat layers are common in the surface 1 m layer. The soil profiles at BN, BR, and DS (**Figs. 3a, 3b, and 3d**) show thick layers of
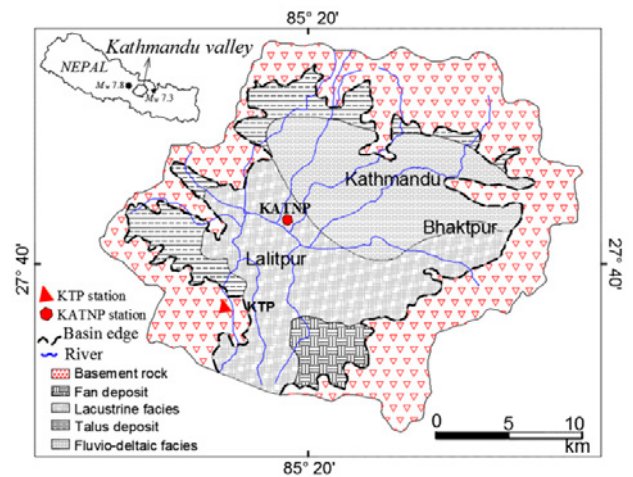
Fig. 2. Geological map of the Kathmandu Valley (modified after Sakai et al., 2002).
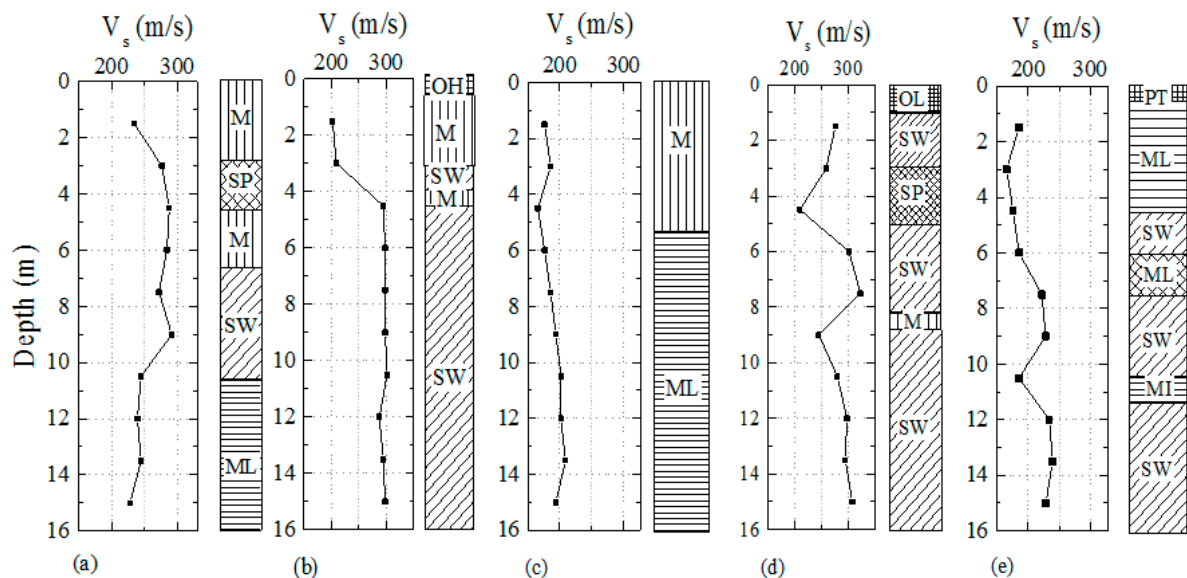
Fig. 3. Shear wave velocity (V_s) and soil classification at five locations in the Kathmandu Valley: (a) Baneshwar (BN), (b) Balkumari (BR), (c) Bauddha (BD), (d) Dhapasi (DS), and (e) Budanilkantha (BT).

well-graded sands and silty sands that are susceptible to liquefaction. The soil profiles at BD and BT (**Figs. 3c and 3e**) show thick and interbedded sandy silts that have high liquefaction resistance. The low plasticity silt with some portion of gravel in underlying layer is found to constitute a PI of 15. However, the plasticity of 23 is found to be occurring in the medium clay slit. As per the grain size distribution in the study area, clays are dominant in most of the sites and a small portion of sandy facies is present in the northern part. The ground water table (GWT) was not determined at the time of site investigation. However, the Kathmandu Valley was in the dry season from March to June 2015, during which the city withdraws a large amount of groundwater; this drew down the GWT of the valley, except in the regions near major rivers.

Paudyal et al. (2012) conducted a seismic micro-termer study in the Kathmandu Valley and found that the resonant frequencies were in the range of 0.5 Hz to 8.9 Hz, with the maximum amplification occurring at about 2 s in the central area due to thick soft sedimentary deposits. However, in addition to amplification at 0.5 seconds (2 Hz), unusual higher spectral amplification was observed in the range of 3 seconds to 6 seconds (0.17 Hz to 0.33 Hz), which could also be due to the complex influence of underlying soft sedimentary deposits in the basin. As the seismicity of Kathmandu Valley is very similar to seismicity

of Mexico City, similar basin effect during 1985 Mexico City earthquake where the ground acceleration was amplified by about 10 times at 2 seconds period due to the presence of lake deposits which resulted in large devastation even at a distance of 300 km from the epicenter (Kramer, 1996).

3.   Ground motions and response spectra

The capability of the network for recording strong ground motions in Nepal is limited. US Geological Survey (USGS) has one seismological station at Kanti Path, Kathmandu (KATNP) and makes the records publicly available. The KATNP station (N: 27.7120°, E: 85.3160°) shown in **Fig. 2** is located at the core of Kathmandu. The KATNP station is located on the top of a thick soft sedimentary soil layer of about 300 m thickness. The V_{s30} at this station is 250 m/s. Another station was installed at Kritipur Municipality Office, Kritipur (KTP) by Tribhuvan University, Nepal, and Hokkaido University, Japan (Takai et al., 2016). The KTP station (N: 27.68216°, E: 85.27259°) shown in **Fig. 2** is located on the rock outcrop at 4.7 km southwest of KATNP station. Both stations located at the place where the damage intensity in the surrounding region was low. The stations do not represent the site conditions of the alluvial deposits where damage
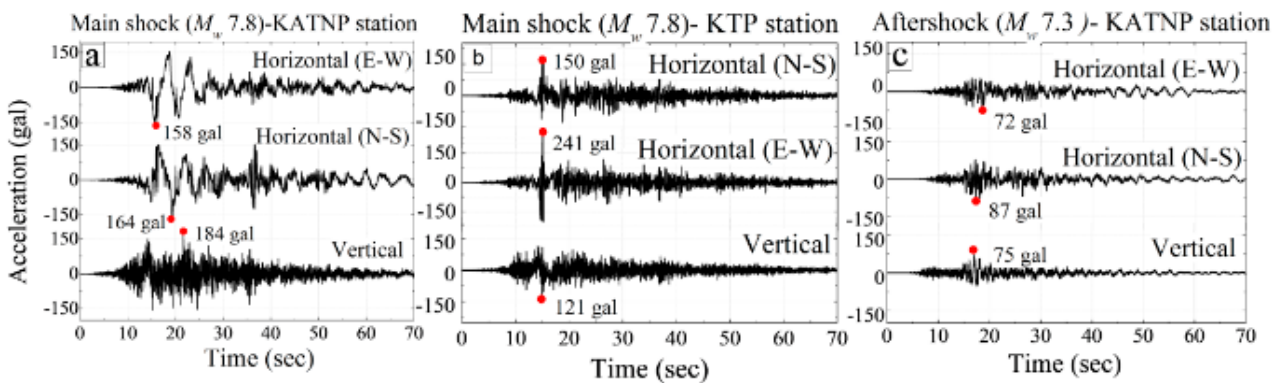
Fig. 4. (a) Accelerograms at KATNP for the M_w 7.8 main shock, (b) accelerograms at KTP (Takai et al., 2016) for the M_w 7.8 main shock, and (c) accelerograms at KATNP for the M_w 7.3 aftershock.
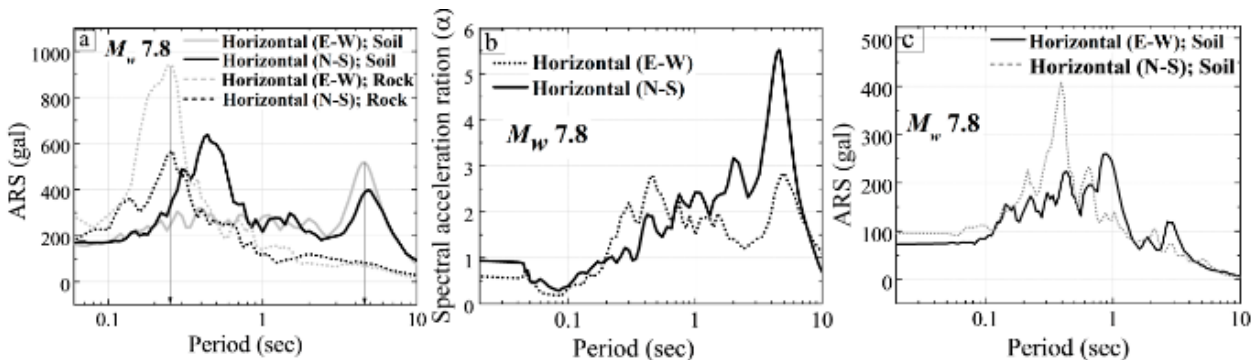
Fig. 5. (a) 5% damped acceleration response spectra (ARS) of the main shock motions at soil (KATNP) and rock (KTP) stations, (b) ARS amplification ratio of the main shock soil motions at KATNP with respect to the outcrop motion at KTP, and (c) 5% damped ARS of the M_w 7.3 aftershock motions at KATNP.

was heavily concentrated; hence the record from this station cannot be used as a representative data for the entire Kathmandu valley.

The E-W, N-S and vertical components of the accelerograms of the main shock at KATNP and KTP are shown in **Figs. 4a** and 4**b**. **Figure 4c** shows the E-W, N-S and vertical components of the accelerograms of the M_w 7.3 aftershock at KATNP. The peak ground accelerations (PGA) of the main shock in horizontal direction are 164 gal (1 gal = 1 cm/s^2) and 241 gal at KATNP (soil site) and KTP (rock site), respectively. Time histories in **Fig. 4a** show that the horizontal accelerograms at KATNP had long duration with conspicuous long-period oscillation at about 5 seconds while the period of horizontal accelerograms at KTP was less than 1 second. This long-period ground motion may be due to the response of the Kathmandu Valley basin. Although the long-period component is large, the shorter-period component (1 second to 2 seconds) is relatively small, resulting in a peak ground acceleration value of 184 gal in vertical directions at KATNP station. The PGA recorded at KATNP station did not exceed the PGA estimates with 10% probability of exceedance in 50 years from the recent regional seismic hazard studies by JICA (2002) and Ram and Wang (2011); however, it is speculated that the local site effects might have contributed to the significant amplification of the motions in Kathmandu Valley and thus make the effects of the earthquake more influential.

The 5% damped acceleration response spectra (ARS) of the main shock at KATNP and KTP are compared in **Fig. 5a.** It is seen that both N-S and E-W components at KTP have a peak at 0.25 seconds while the N-S component at KATNP has two prominent periods at 0.47

s and 5 s and E-W component has one peak at 5 seconds. The acceleration records at soil site (KATNP) are broadband and contain the long-period components at 5 s. The features of the ground motions are the result of the effects of the thick, soft sediment in the valley, where the KATNP was built upon. The horizontal components of the main shock and aftershock show the similar characteristics when the period is less than 1 second (**Figs. 5a and 5c**). In contrast with horizontal components of main shock at KATNP, aftershock components do not show the peaks at 5 seconds. The peaks at about 5 seconds of the main shock components at KATNP may be attributed to the main shock sources rather than the local site effects.

To understand the site effect on the main shock motions, spectral acceleration ratios (KATNP/KTP) of the two main shock motions, presented in **Fig. 5b** for each horizontal component, represent the amplification effect of the deep alluvial soil on the ground motion. It is shown that the ground motions at the KATNP site were strongly influenced by the local site condition at long periods. These spectral ratios reveal that spectral response at the soft soil site is amplified by a factor varying between 1.5 and 4.5 compared to the rock site in the period range of 0.3 seconds to 5.0 seconds. The fundamental periods of the heavily damaged residential buildings and heritage structures on the alluvial basin in Kathmandu Valley fall into this range. **Figure 5c** shows the 5% damped ARS of the aftershock at KATNP. N-S components of aftershock at KATNP has a peak at 0.35 seconds while the E-W components at 1 second. Both E-W and N-S components of main shock have the secondary peaks at about 5 seconds whereas the aftershock components do not show
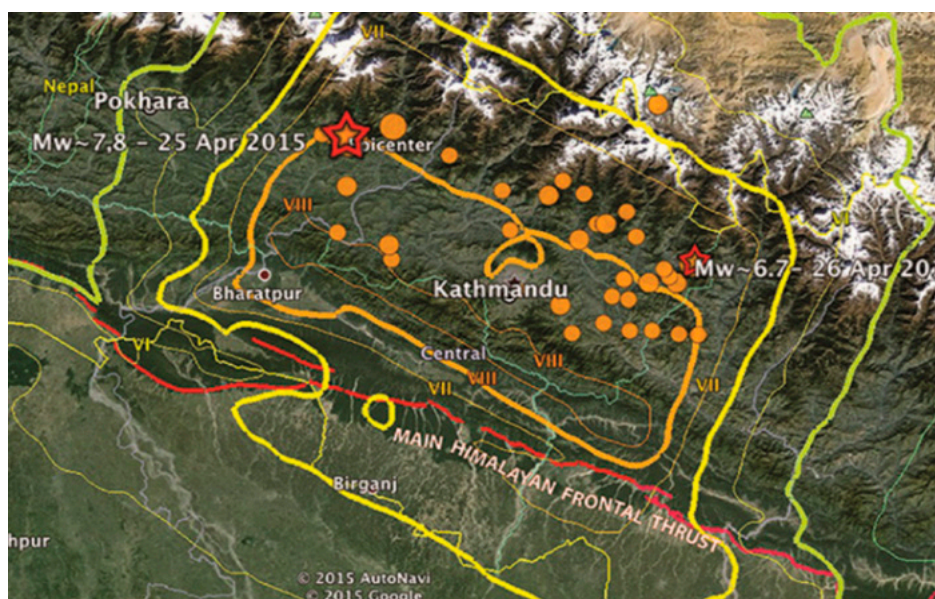
Fig. 6. Isoseismal map for the 2015 Gorkha Nepal earthquake (USGS, 2015).
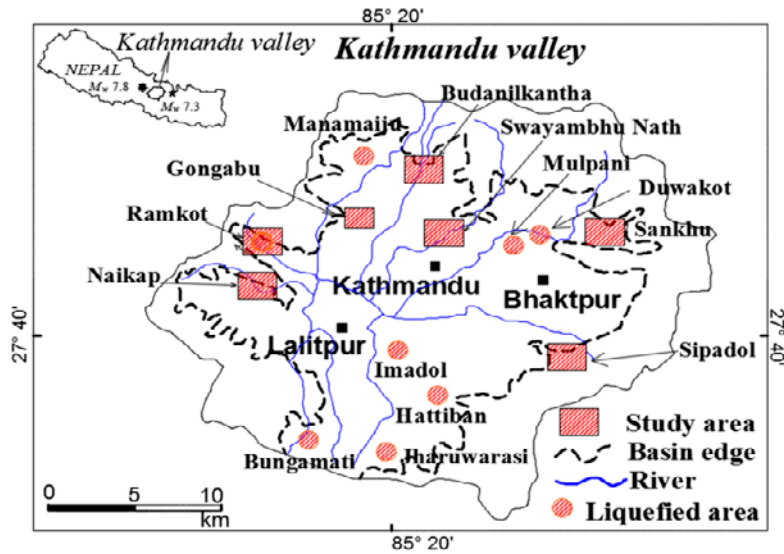
Fig. 7. Locations of the study areas for local site effects and liquefaction.

the peaks at 5 seconds. Details of the characteristics of ground motions recorded during the Gorkha earthquake can be found in Parajuli and Kiyono (2015) and Sharma et al. (2016).

4.   Effect of Local Geology and Topography

The earthquake shaking intensity depends not only on magnitude and distance to the epicenter but also on local soil conditions and topography. However, in a single earthquake, shaking at one site can easily be 10 times stronger than at another site, even when their distance from the ruptured fault is same (Geli, 1988; Aki, 1993). The earthquake intensity was sporadically high, attaining a maximum of MMI VIII at certain places. Intensity VIII was observed in Kathmandu due to non-engineered construction on thick soft soil or near the river plain. Most of the affected region experienced MMI VII or less shaking. The spatial distribution of the intensity and isoseismal map for the 2015 Gorkha Nepal earthquake, based on the damage survey, is given in **Fig. 6**. Analysis of isoseismal map reveals that some of the localities have higher intensity as compared with the surrounding. The distribution of the damage within Kathmandu is particularly of interest for site effects investigation. Regarding the damage experienced by the structures, the Kathmandu Valley can be subdivided into two zones. First zone is a newly deposit alluvium, or filled soil, where a majority of the heavily damaged or collapsed structures were located. The second zone is located along the edge of the Kathmandu Valley basin where heavily damaged structures as well liquefaction were

Fig. 8. Damaged buildings at (a) Gongabu(N: 27.738114°, E: 85.307635°), (b) Machhapokhari (N: 27.735511°, E: 85.305340°), (c) Newly constructed building at Tripureshwar, Kathmandu along the Tukucha River and (b) severe diagonal cricks on the wall (N: 27.691972°, 85.316163°).

located. This section illustrates case studies in the areas where these effects were observed.

4.1 Soft soil effects

Though the Kathmandu Valley is about 80 km away from the epicenter, it experienced a shaking intensity higher than the regions around the epicenter. Kathmandu, with a zone factor 1.0 according to the Nepal seismic code NBC 105 (NBC, 1994) is expected to experience PGA value (0.3 g) higher than the recorded value (0.18 g) as mentioned in the previous section. From the structural
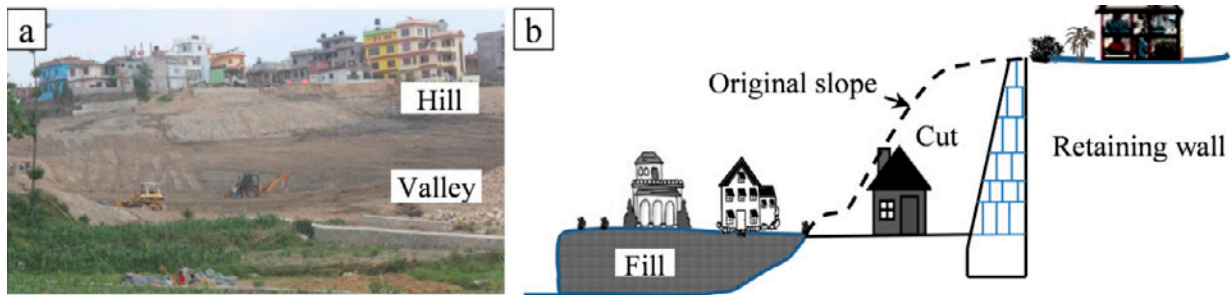
Fig. 9. (a) Earthwork activities for housing construction in the Kathmandu Valley (N: 27.698884°, E: 85.366282°), and (b) schematic diagram of the cut and fill. Building structures on the hill were considered intact (Sharma and Deng, 2017).

Fig. 10. Performance of a RC building on new fill at (a) Purano Naikap (N: 27.700051°, E: 85.264569°), Kathmandu and (b) Balaju (N: 27.742651°, E: 85.300751°).

damage evaluation, it has been found that the damage was concentrated in a few pockets of the Kathmandu valley, such as Gongabu, Balaju, Machha Pokhari, Ramkot, Naikap, and the surrounding areas in the Kathmandu Valley (Hazarika et al., 2016). From the observation the effect of loose fill and young deposits were evident from the extensive structural damages and failures at these sites. Most four and five-storey reinforced concrete (RC) buildings in this region experienced severe damage or failure (Sharma et al., 2016). Since these RC buildings have the predominant period of approximately 0.5 seconds, the severity may be attributed to the predominant period of 0.45 seconds (**Fig. 5a**) of the horizontal component of the main shock.

Figure 7 shows the areas selected to investigate the effects of local soil characteristics on the structural damage of buildings. The case histories in Gongabu and Machhapokhari, along the Bishnumati River where maximum damage to RC buildings occurred, are particularly of interests for local soil effect investigation. The geological map of Gongabu and Machhapokhari show that both areas lie on recent (Holocene) alluvium soil. The recent alluvium near the river mainly consists of sand and silt, with a shallow ground water table, typically 1.5 m to 3.0 m from ground surface. The standard penetration test (SPT), N values are mostly lower than 15. From the preliminary study of the Gongabu and Machha Pokhari site, it is indicated that the soil is very soft (Holocene alluvium) and water logged, which can amplify the seismic wave and therefore increase the severity of the damage to buildings.

Figures 8a and 8b show typical building failure at Gongabu and Machha Pokhari. Similar cases of local soil effects can be found along the major river channel in the Kathmandu Valley. **Figure 8d** shows sever cracking on the wall of a well-engineered, newly constructed building at Tripureshwar along the Tukucha River (**Fig. 8c**). It also may be inferred that soil amplification of lower frequency ground motion along major rivers in Kathmandu caused greater damage to buildings, probably due to double resonance effects (resonance at 0.25 seconds and 4.5 seconds; **Fig. 5a**) (Graves, 1996).

The destruction of building structures supported on shallow foundations in Ramkot, Naikap and Sipadol (locations labeled in **Fig. 7**) could be interpreted as local site amplification, because most of these structures were constructed on loosely compacted fill. The organic soft fill was originated from the cut of adjacent hill as shown in **Fig. 9**. The fill was not compacted enough to achieve high density and strength of filled soil. On the contrary, many building structures on the hill top were not damaged as severely as the structures on the fill because the intact hill soils were generally stiff and thus the shaking amplification may not be significant. **Figure 9b** illustrates the schematic diagram of the land preparation for houses in Kathmandu Valley. **Figure 10** shows the performance of a RC building, which is designed for earthquake resistance, developed on loosely compacted fill. This highlights the importance that local site effects need to be considered in design.

4.2 Basin effects

As the waves pass from harder to softer rocks and slow down, the amplitude of the waves may be amplified to carry the same amount of energy. Thus, shaking amplitude tends to be stronger at sites with softer surface layers, which is usually in the basin of a valley where seismic waves propagate from the hard rock across the soft soil sediment. This effect is termed as the basin effect. **Figures 4 and 5** clearly highlight the amplification of

Fig. 11. (a) Park View Horizon apartment (N: 27.739762°, E: 85.324410°) was severely devastated by the main shock due to the basin effect, and (b) close view.

ground motion due to soft soil sediment in Kathmandu Valley.

The effect of low frequency amplification caused by the Kathmandu Valley basin is evident from the severe damage to well-designed tall buildings in Kathmandu. It was observed that the majority of one- and two-storey masonry houses, constructed more than 50 years ago, were intact, while new multi-storey buildings collapsed due to the failure of the ground floor columns. The scattering of failed multi-storey buildings throughout the cities of Kathmandu, Bhaktapur, and Lalitpur implies that the damage may not be purely attributed to the poor quality construction materials or inadequate design, because similar apartment buildings with fewer stories were observed to experience much lesser damage. It is inferred that amplification of long-period ground motion (**Fig. 4**) due to the soft deep valley sediment might have caused greater damage to the multi-storey buildings than the short ones.

Although newly constructed high-rise apartment buildings are considered as a well-engineered building type in Nepal, severe cracks were found on many infill walls of this type of buildings. It was found that out of 15 newly constructed high-rise apartment buildings in Kathmandu Valley, 11 were severely affected by the earthquake. **Figure 11** shows a 16-storey, apartment complex, Park View Horizon, which exhibited many major cracks along its height. Non-structural burnt bricks were used as the infill material, which led to a significant increase in weight. In contrast to a well-engineered high rise apartment, old and poorly constructed residential buildings around the apartment were found intact (**Fig. 11a**).

Another case that highlights the soft soil effect is the newly constructed high-rise building in Buddhanagar, Kathmandu, as shown in **Fig. 12**. The high-rise building is located in between several old masonry and non-engineered RC buildings. The high-rise buildings were well engineered while the residential houses (RC or masonry) are old and poorly constructed; however, the apartment suffered from more severe damage than the old short buildings. This case history shows that the effect of long period ground motion due to newly deposit sediments

Fig. 12. High rise building at Buddhanagar, Kathmandu (N: 27.682565°, E: 85.329619°).
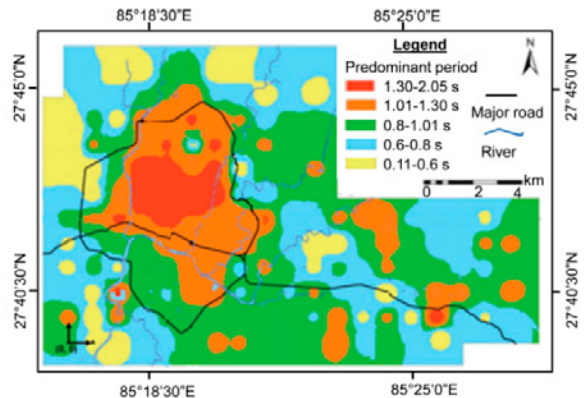
Fig. 13. The contour map of predominant period of ground of the Kathmandu region (Paudyal et al. 2012).
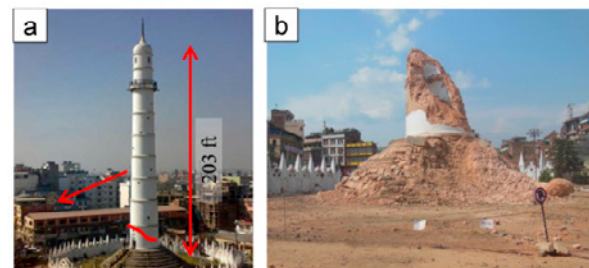
Fig. 14. (a) Dharahara tower before earthquake, and (b) base of Dharahara remaining after earthquake (N: 27.70082°, E: 85.31249°).

Fig. 15. Almost completely destroyed old town at (a) Madhyapur Thimi, Bhaktpur (N: 27.678854°, E: 85.404766°) and (b) Balaju, Kathmandu (N: 27.736054°, E: 85.302531°).

Fig. 16. Multi-tiered Pagoda style temples (N: 27.704226°, E: 85.306222°) (a) before earthquake (b) after earthquake.

along the Bagmati River exacerbated the destruction of tall RC buildings that have long predominant periods.

The fundamental time period of multi-storey RC buildings can be approximated as $0.075h^{0.75}$, where h is the height of buildings in meter (IS 1893, 2002). Hence, buildings of (3-5) storey height possess fundamental time period in the range of 0.3 seconds to 0.6 seconds. Causes of the major damage in well-engineered multi-storey apartment buildings in Kathmandu Valley may be attributed to the long-period ground motions as shown in the spectra of **Fig. 5**, which shows a predominant period ranging from 0.3 seconds to 0.6 seconds. Tall buildings with long predominant periods are expected to be more vulnerable to long-period ground motions than short buildings with short predominant periods. Similar basin effects were observed in Los Angeles during the 1994 Northridge earthquake, and in Mexico City during 1985 earthquake. The San Fernando and Los Angeles basins, containing alluvial deposits, experienced high site response factors due to the amplification of the ground motion and the focusing effect of the valley (USGS, 1996).

The predominant period of the ground in Kathmandu valley changes abruptly within a short distance due to the variability in the sediment thickness and its properties (Paudyal et al., 2012). The contour map of the dominant period of ground of the Kathmandu region is shown in **Fig. 13**. These predominant period contours provide some valuable information which can be roughly correlated with the period of the damaged structures. Failure of the Dharahara tower, a 203 feet tall unreinforced masonry tower (**Fig. 14**), could also be related to the long-period dominance in the central region (1.30 seconds to 2.05 seconds).

The old unreinforced masonry buildings in Balaju, Kathmandu and Madhyapur Thimi Bhaktpur (**Fig. 15**), generally fall under the acceleration-sensitive region of the spectra, with a period range of 0.1 seconds to 0.6 seconds, which closely matches with the predominant period of ground of the affected region (0.11 seconds to 0.80 seconds). Multi-tiered temples had suffered severe damage during the earthquake at Kathmandu Durbar Square. Some of them completely collapsed and were reduced to rubble. The Natural period of the multi-tiered Pagoda style temple lies between 1.0 second to 3.0 seconds (Parajuli and Kiyono, 2015), which closely coincides with the predominant period of ground of the Kathmandu durbar square. This resulted complete collapse of many multi-tiered Pagoda style temples at Kathmandu durbar square (**Fig. 16**) (KC et al., 2017). Thus, the construction of new buildings should be regulated based on the study of soil dynamics.

Fig. 17. (a) Ridge-top damage interpreted from satellite image decorrelation before and after the main shock (ARIA/JPL-Caltech), (b) a completely destroyed school on the hill top (N:27.837392°, E:85.854154°), and (c) an intact school at the hill valley near the school on the hill top (N:27.804319°, E: 85.913725°) (Sharma and Deng, 2017).
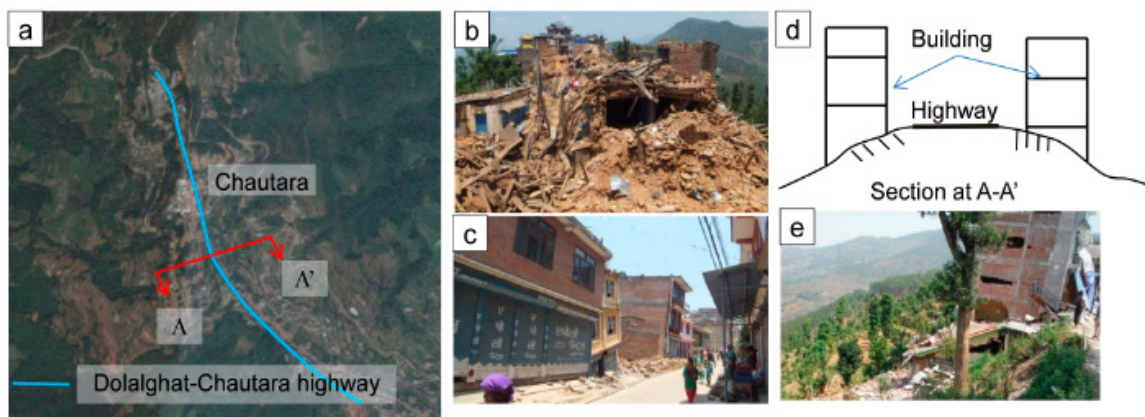
Fig. 18. (a) Chautara on the top of ridge (N: 27.776336°, E: 85.712683°) (b) schematic cross-section about A-A', (c) severe damage of the buildings at Chautara, (d) and (e) damage on buildings located on slope ground.

4.3 Topographic (ridge) effects

Topography effects refer to the amplification of ground shaking at topographic convex, such as hills, ridges, and cliffs, due to the energy-focusing effect. This topographic feature can significantly alter the intensity, frequency content, and duration of ground shaking compared to the shaking that would have experienced had it been on a flat surface (Sanchez-Sesma et al., 1985). The damages during 1995 Greece earthquake were concentrated in the central elevated part of the town, whereas the flat coastal region remained almost intact. (Athanasopoulos et al., 1999). Extensive damage was observed on the ridges of Canal Beagle during the 1985 Chile earthquake. The ridge effects were explicitly observed based on distinctively different severity of damage to buildings on the hills and in the nearby valley.

Figure 17a shows the damage distribution (source: ARIA/JPL-Caltech 2015) of building in the hilly areas of Nepal. Red and yellow represent completely damage and partially damage buildings respectively. It is shown that the severe damages are aligned with the ridge lines. **Figures 17b and 17c** compare the seismic performance to two similar schools building constructed in the same era (about 50 years ago) near the epicenter of the M_w 7.3 aftershock. The school building in the nearby valley performed very well, while the school building located on the top of a hill was completely demolished. The distinctive performance of the school buildings could be explained by the ridge effect. The collapse of the building on the hill top was attributed to the ground motion amplification by the hill.

Chautara town is one of the places that suffered the most severe damages during the earthquake (**Fig. 18**). The town is located along Arniko highway on the mountain ridge (**Fig. 18a**). The damage to the Chautara town (**Figs. 18b, 18d and 18e**) was very severe though it is far from the epicenter and earthquake fault. The reason can be the amplification of narrow mountain ridge. The field investigations in Chautara also show that a majority of the damaged buildings, mostly mid-rise reinforced concrete (RC) moment-frame systems, were located on steep slopes along the Arniko highway (**Figs. 18d and 18e**). In contrast,
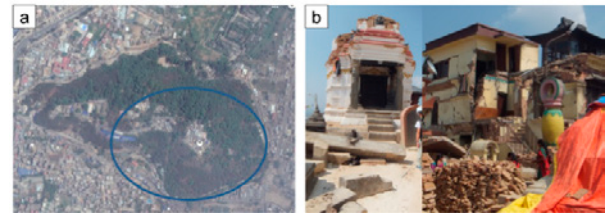
Fig. 19. (a) Swayambhu Nath, a small hill in the center of Kathmandu Valley, and (b) severely destructed buildings (N: 27.714980°, E: 85.290401°) at the hill top of Swayambhu Nath.

building with the same structural characteristics located on flat ground did not suffer much damage.

Ridge effects were also observed in the Kathmandu Valley. Building damage was specifically concentrated at the top of an isolated hill at Swayambhu Nath as shown in **Fig. 19**. The location of the hill is labeled in **Fig. 7**. It was noticed that the shake intensity was so high at the hill top that many buildings at the top were severely destructed or destroyed (**Fig. 19b**). On the contrast, buildings in the lowland surrounding Swayambhu Nath were not significantly damaged.

A damage survey of the structures in rural areas, focusing on the topographic effect on structural damage, had been completed a few months after the Gorkha earthquake. The site for the survey was chosen in the Harmi VDC, Gorkha district, about 17 km southwest from the epicenter of the Gorkha earthquake 2015. A contour map of the surveyed area was developed as shown in **Fig. 20.** A total of 149 structures in the strip of a small mountain slope were studied and ranked in the range of damage index from 0-5. Structures were also categorized as small, medium and large based on their floor level and plinth area. Structures having less than 45 m² plinth area are categorized as small, where up to 75 m² and more are taken as medium and large respectively. Heavily damaged structures with damage grade 5 were not spotted but grade 4 structures were 6%, similarly 24% of structures fall in damage grade 3 and grade 2 each. A maximum, 38% of the structures in the study area had damage grade of 1 along with no damage or minor damage structures with grade 0 were at 8%. It was found that most of the
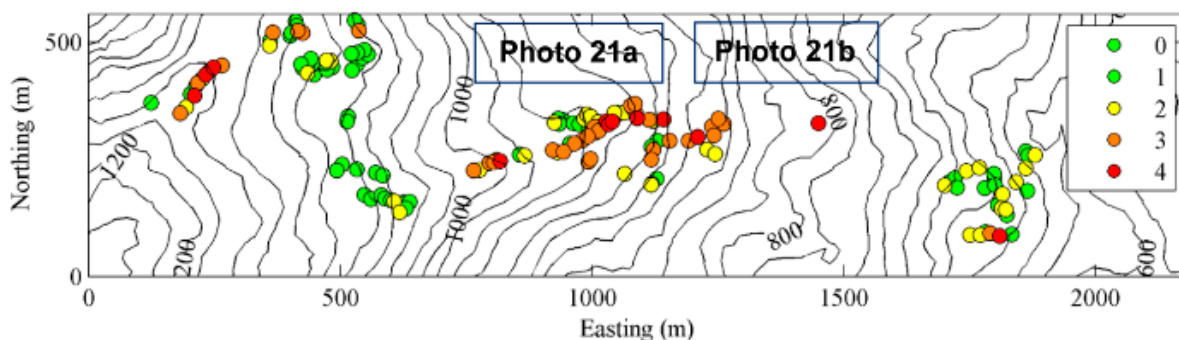
Fig. 20. Damage scenario in mountainous area with the contour map (N: 28.088225°, E: 84.542748°) (Parajuli and Kiyono, 2015).

structures in ridge line suffered more damage than those located in the slopes (**Fig. 21a**). When we only consider the structures located in the local ridge line, a total of 52%, 15%, 19%, 52% and 14% of the structures categorized with damage grade of 1, 2, 3 and 4. There were not any structures having grade 0 in ridge line. Structural system of all the structures were similar, with almost the same source of materials. When we look at the differences between similar structures, but having different damage grades, we found two major reasons for reducing the damage level. One of the major reasons was cement plaster/pointing in the main wall. Almost all of the structures with cement plaster were not heavily damaged. Those structures had enormous cracks, however did not collapse, as like the one shown in **Fig. 21b**. This study of a small village clearly highlights the topographic (ridge) effects on the damage severity of the structures (Parajuli and Kiyono, 2015).

In Nepal, school building and temples are often constructed on hilltops. Many of these structures located on the top of hills were destructed (**Fig. 22**), which can be attributed to topography amplification effects.

Fig. 21. (a) Stone masonry building, a residential house collapsed on the ridge line and (b) cracks on the wall of the building located on the ridge line.
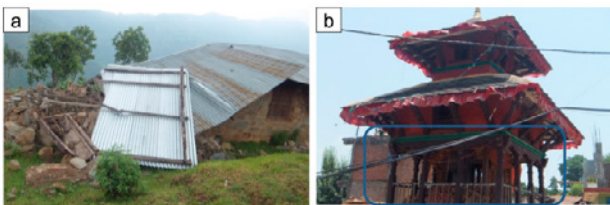
Fig. 22. (a) School on the top of hill at Harmi, Gorkha (N: 28.089571°, E: 84.542719°) (b) temple on the top of hill at Chautara (N: 27.774824°, E: 85.715495°).
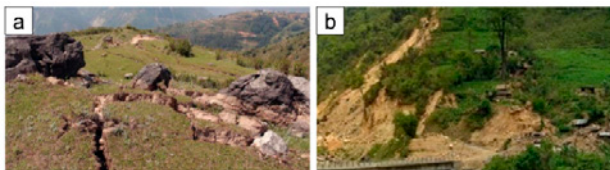
Fig. 23. (a) Large ground fissures on the top of hill (Photo: O. Marc, GFZ) and (b) Slope failure near the epicenter along the Abu Khairahani-Barpak road (N: 28.170481°, E: 84.706223°).

A large number of steep slopes failed at shallow depth in the epicentral area, and their scale in terms of quantity and dimension tends to increase toward the epicentre. Slope failure concentration along midslopes with aspects in the fault-normal direction, indicating the rupture directivity effects. Ground fissures and numerous slope stability failures were observed at the hilltops and along ridge (**Fig. 23a**), especially in the case of elongated ridges with steep slopes, showing the strong indication of the topographic amplification (Sharma, 2016). In some cases, damage was observed on one side of the ridge slope, but not on the other. This occurrence may be attributed to the use of heavy equipment, and destruction of the toe for road construction, that created a weakness in the direction of total collapse (**Fig. 23b**).

4.4 Basin edge effects

The basin edge effect is the amplification of seismic energy at the margins of sedimentary deposits. This leads to the generation of a surface wave at the edge of sedimentary deposits, creating two dimensional resonances. When such sediments are laterally confined by a more rigid basement rock, as in the Kathmandu Valley, the seismic behaviour becomes multi-dimensional (Iyisan and Khanbabazade, 2013). The basin edge effect was profoundly noticed during the 1995 Kobe earthquake in Japan (Kawashe, 1996) where it was found that the heavily damaged structures were concentrated along the basin edge. The town Dinar, most affected from the 1995 Dinar, Turkey earthquake, was located at the edge of an alluvial basin (Bakir et al., 2002).

Severe damages were observed adjacent to basin edges around the Kathmandu Valley after the main shock and subsequent aftershocks. This is evidence that basin edge effects had an impact on the performance of buildings because of the geological features of the Kathmandu Valley. The increase of the amplification when compared to the case of horizontal layering in the valley center may be a factor of 5 to 10. The motion amplification also depends on the velocity contrast between the layers and the geometry of the basin (Iyisan and Khanbabazade, 2013).
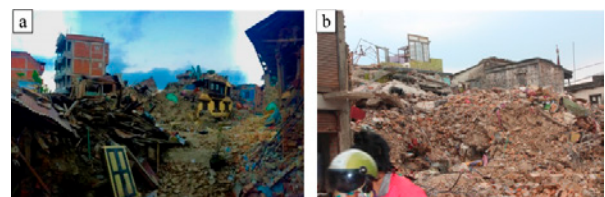
Fig. 24. Severe damages of buildings at (a) Sankhu (N: 27.513595°, E: 85.329142°) and (b) Balaju, Kathmandu (N: 27.735512°, E: 85.301820°).
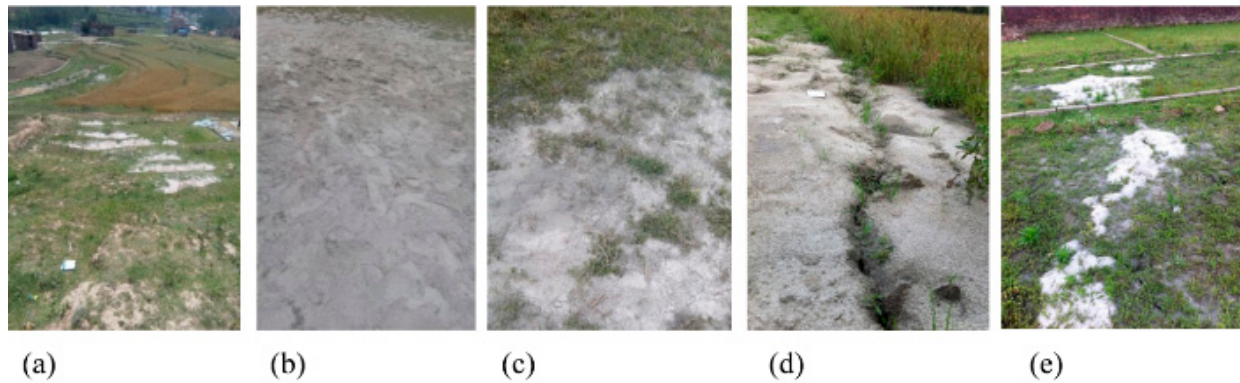
Fig. 25. Liquefaction along the basin edge of Kathmandu Valley (a) Ramkot, Kathmandu, (b) Manamaiju, Kathmandu, (c) Duwakot, Bhaktpur, (d) Bungamati, Lalitpur, and (e) Mulpani, Bhaktpur.

When looking at the damage distribution caused by the Gorkha earthquake, one can easily notice severe damage along the basin edges of the Kathmandu Valley. **Figure 7** shows several severely damaged towns within the valley. Towns such as Duwakot, Kapan, Manmaiju, Budhanilkantha, Jorpati, and Sankhu located at the edge of the valley basin were severely affected (Sharma and Deng, 2016) as compared to other old towns with many non-engineered masonry buildings, such as Asan and Patan located in the center of the Kathmandu Valley. On the other hand, most of the old structures were destructed and new RC structures were severely damaged in the towns near the basin edge (**Fig. 24**). The observed damage distribution and high intensity of the ground shaking near the basin edge clearly demonstrated the influence of the basin-edge effect.

Liquefaction triggered by the 2015 Gorkha earthquake appears to be fairly limited and localized (Subedi et al., 2016; Sharma, 2016). The localized areas where liquefaction was observed are Manamaiju, Ramkota, Bungmati, Jharuwarasi, Hattiwan, Imadol, Mulpani and Duwakot (**Fig. 7**). Most of liquefied sites are either within or on the edges of the Kathmandu Valley. These are regions likely to be more vulnerable to liquefaction due to basin edge effect; however, liquefaction potential analysis of the liquefied areas is needed to get into real scenario. **Figure 25** shows some examples of liquefaction occurred along the edge of Kathmandu basin.

5. Conclusions

This paper investigates the local site effects during the 2015 Gorkha earthquake that struck Nepal on April 25, 2015, followed by a series of aftershocks. The following observations and conclusions can be drawn.

1. The peak ground acceleration at a soil site in the Kathmandu Valley in horizontal direction was 184 gal. The ground motions contained long-period components at the predominant period of 0.47 seconds and a secondary period of 5.0 seconds. Comparison of the recorded ground motions at soil and outcrop rock sites shows a significant amplification of the response spectra at the period of 5.0 seconds, due to the soft, deep sediments in the valley.

2. The damage patterns revealed strong influence of local site conditions on the severity of the damage at many places. Building damage in the Kathmandu Valley and nearby villages was caused not only caused by the poor quality of non-engineered buildings, but also by local site effects induced by soft alluvial soil deposits, ridge effects and basin effects.

3. Local soil properties had significant impacts on the damage intensities of building structures. Building structures developed on young, unconsolidated Holocene deposits showed more extensive damages than structures on old Pleistocene deposits at the same region. Buildings on loose fill were observed to be more vulnerable than structures on the adjacent hill top.

4. Severe damage to well-engineered high-rise buildings than to old and non-engineered short buildings highlights the effect of long-period ground motion due to basin effects.

5. Ridge effects were observed through the distinctive performance of two school buildings. One school building being destroyed on the hill top and the other remaining functional on the hill valley. Ridge effects on building performance were also noticed in the Kathmandu Valley, which is generally flat but still contains several topographic hills.

6. Basin edge effects were noticed by comparing the distribution and intensity of building damages and liquefactions in the Kathmandu Valley and on edges of the basin. More severe damages on non-

engineered and well-engineered buildings were observed along the basin edges.

7. The USGS station KATNP lies in the central area of the valley with long-period dominance; hence the record from this station cannot be used as a representative data for the entire Kathmandu Valley and nearby regions. Thus, for better understanding of the seismicity of the region, strong motion stations should be set up at numerous locations.

8. This study revealed the importance of carefully considering site conditions such as soil types and topography, a factor that has not been considered in the Nepal Building Code. Making risk maps for site effects contributes largely to the risk reduction of earthquakes, e.g. the decision-making about urban planning in earthquake-prone areas.

Acknowledgement

References

Aki, K., 1993. Local site effects on weak and strong ground motion. Tectonophysics, **218** (1-3):93-111.

Ambraseys, N.N. and Douglas, J., 2004. Magnitude calibration of north Indian earthquakes. Geophysics Journal International, **159**:165-206.

Athanasopoulos, G.A., Pelekis, P.C. and Leonidou, E.A., 1999. Effects of surface topography on seismic ground response in the Egion (Greece) 15 June 1995 earthquake. Soil Dyn. Earthq. Engrg., **18**: 135-149.

Bakir, B.S., Ozkan, M.Y. and Ciliz, S., 2002. Effects of basin edge on the distribution of damage in 1995 Dinar, Turkey earthquake Soil Dyn. Earthq. Engrg., **22** (4):335-345.

Bilham, R., Gaur, V.K. and Molnar, P., 2001. Himalayan Seismic Hazard. Science, **293**:1442-1444.

Celebi, M., 1987. Topographical and geological amplifications determined from strong-motion and aftershock records of the 3 March 1985 Chile earthquake. Bull. Seismol. Soc. Am., **77**: 1147-1167.

Copeland, P., 1997. The when and where of the growth of the Himalaya and the Tibetan Plateau. In: Ruddiman, W.F. (Ed.), Tectonic Up lift and Climate Change. Plenum Press, New York: 19-40.

Dahal, R.K., 2006. Geology for Technical Students. Bhrikuti Academic Publications, Kathmandu, Nepal: pp 756.

Dixit, A., Dwelley-Samant, L., Nakarmi, M., Pradhanang, S. and Tucker, B., 2000. The Kathmandu Valley earthquake risk management project: an evaluation. Proc. of 12th World Conference on Earthquake Engineering, Auckland, New Zealand, Paper 0788.

Geli, L., Bard, P.Y. and Jullien, B., 1988. The effect of topography on earthquake ground motion: a review and new results. Bull. Seism. Soc. Am., **78**: 42-63.

Graves, R.W., 1996. Simulating seismic wave propagation in 3-D elastic media using staggered grid finite difference. Bull. Seismol. Soc. Am., **86**: 1091-1107.

Hazarika H., Bhandary, N.P., Kajita, Y., Kasama, K., Tsukahara, K. and Pokharel R.K., 2016. The 2015 Nepal Gorkha Earthquake: An overview of the damage, lessons learned and challenges. Lowland Technology International Journal, Special Issue on: Nepal Earthquake & Disaster, **18** (2): 105-118.

Hough, S.E. and Bilham. R., 2008. Site response of the Ganges basin inferred from re-evaluated macroseismic observations from the 1897 Shillong, 1905 Kangra, and 1934 Nepal earthquakes. Journal. Earth. Syst. Sci., **117** (S2): 773-782.

Hough, S.E., Altidor, J.R., Anglade, D., Given, D., Janvier, M.G., Maharrey, J.Z., Meremonte, M., Mildor, B.S., Prepetit, C. and Yong, A., 2010. Localized damage caused by topographic amplification during the 2010 M 7.0 Haiti earthquake. Nat. Geosci., **3**: 778-782.

IS 1893 (Part 1), 2002. Criteria for earthquake resistant design of structures, General provisions and buildings (Fifth revision), Bureau of Indian standards, New Delhi: pp 24.

Iyisan, R. and Khanbabazade, H., 2013. A numerical study on the basin edge effect on soil amplification. B. Earthq. Engrg., **11** (5): 1305-1323.

Japan International Cooperation Agency (JICA), 2002. "The study of earthquake disaster mitigation in the Kathmandu Valley, Kingdom of Nepal, Final Report I-IV.

Kawase, H., 1996. The cause of the damage belt in Kobe: "The basin-edge effect," constructive interference of the direct S-wave with the basin-induced diffracted/Rayleigh waves, Seism. Res. Lett., **67** (5): 25-34.

KC, A., Sharma, K. and Pokharel, B. 2017. Performance of heritage structure in Kathmandu Valley during 2015

Gorkha Nepal earthquake, Intl. J. Archit. Herit. (Submitted).

Kramer, S., 1996. Geotechnical Earthquake Engineering. Prentice-Hall, Upper Saddle River, NJ, USA: 309-319.

Manandhar, S., Hino, T., Soralump, S. and Francis, M., 2016. Damages and causative factors of 2015 strong Nepal Earthquake and directional movements of infrastructures in the Kathmandu Basin and along the Araniko Highway. Lowland Technology International Journal, Special Issue on: Nepal Earthquake & Disaster, **18** (2): 141-164.

Mugnier, J.L., Huyghe, P., Gajurel, A.P., Upreti, B.N. and Jouanne, F., 2011. Seismites in the Kathmandu basin and seismic hazard in central Himalaya. Tectonophysics, **509** (1-2): 33-49.

National Seismological Center of Nepal (NSC), 2016 http://www.seismonepal.gov.np/index.php (accessed on September 1, 2016).

Nepal National Building Code (NBC)-105, 1994. Nepal national building code for seismic design of buildings in Nepal, ministry of housing and physical planning, Department of Buildings, Kathmandu, Nepal: pp 14.

Pandey, M.R. and Molnar, P., 1988. The distribution of intensity of the Bihar-Nepal earthquake 15 January 1934 and bounds of the extent of the rupture zone. J. Nepal Geological Society, **5**: 22-44.

Parajuli, R. R., and Kiyono, J., 2015. Ground motion characteristics of the 2015 gorkha earthquake, survey of damage to stone masonry structures and structural field tests. Front. Built Environ., **1**: pp 23.

Paudyal, Y.R., Bhandary, N.P. and Yatabe, R., 2012. Seismic microzonation of densely populated area of Kathmandu valley of Nepal using microtremor observations. J. Earthq. Engrg., **16** (8): 1208-1229.

Ram, T.D. and Wang, G., 2011. Probabilistic seismic hazard analysis in Nepal. Earthq. Engrg. Engrg. Vib., **12**: 577-586.

Rayhani, M.H.T., El Naggar, M.H. and Tabatabaei, S.H., 2008. Non-linear analysis of local site effects on seismic ground response in the bam earthquake. Geotech. Geol. Engrg., **26**: 91-100.

Sakai, H., Fujii, R. and Kuwahara, Y. 2002. Changes in the depositional system of the Paleo-Kathmandu Lake caused by uplift of the Nepal Lesser Himalayas. J. Asian Earth Sci., **20**: 267-276.

Sánchez-Sesma, F.J., Bravo, M.A. and Herrera, I., 1985. Surface motion of topographical irregularities for incident P, SV and Rayleigh waves. Bull. Seismol. Soc. Am., **75**: 263-269.

Sharma, K. and Deng, L., 2016. Geotechnical Engineering Aspect of the April 25, 2015, Gorkha, Nepal earthquake. The 1st Intl. Symp. on Soil Dynamics and Geotechnical Sustainability Aug 7-9, 2016 Hong Kong: 70-73.

Sharma, K. and Deng, L., 2017. Geotechnical Engineering Aspect of the April 25, 2015, Gorkha, Nepal earthquake. J. Earthq. Engrg. (accepted).

Sharma, K., 2016. Field reconnaissance after the April 25, 2015 M_w 7.8 Gorkha earthquake. Proc. of 1st NESA Symposium, University of Alberta, Alberta, Canada: II (7-8).

Sharma, K., Deng, L. and Noguez, C.C., 2016. Field investigation on the performance of building structures during the April 25, 2015, Gorkha earthquake in Nepal. Engrg. Struct., **121**: 61-74.

Subedi, M., Acharya, I.P., Sharma, K. and Kalpana, A., 2016. Liquefaction of Soil in Kathmandu Valley from the 2015 Gorkha, Nepal, Earthquake. Nepal Engineers' Association, Technical Journal- Special Issue on Gorkha Earthquake 2015, XLIII-EC (1): 108-115.

Takai, N., Shigefuji, M., Rajaure, S., Bijukchhen, S., Ichiyanagi, M., Dhital, M.R. and Sasatani, T., 2016. Strong Ground Motion in the Kathmandu Valley during the 2015 Gorkha, Nepal, Earthquake. Earth Planets and Space, **68**: pp 10.

United States Geological Survey (USGS) (1996) http://pubs.usgs.gov/of/1996/ofr-96 0263/localef f.htm.

United States Geological Survey (USGS), 2015. http://earthquake.usgs.gov/realtime/product/finite-fault/us 20002926/us/1429969841288/20002 926.html (accessed on May 27, 2015).

Villaverde, R., 2008. Fundamental concepts of earthquake engineering. Taylor & Francis Groups: CRC Press: pp 298.